THE ANNALS OF "DUNAREA DE JOS" UNIVERSITY OF GALATI
FASCICLE XI – SHIPBUILDING. ISSN 1221-4620
2016

NUMERICAL PREDICTION OF THE PERFORMANCES OF A NON-CAVITATING PROPELLER WORKING IN OPEN WATER

Adrian Lungu
"Dunarea de Jos" University of Galati
Faculty of Naval Architecture
Domneasca Street, No. 47, RO-800008, Romania
E-mail:adrian.lungu@ugal.ro

ABSTRACT

The present study describes a 3D numerical simulation of the viscous flow around a five blade propeller model, as an intermediate step in developing a robust technique for a further investigation of the flow around a self-propelled ship hull. Several computations are performed by using either the FINE^{TM}/Marine component of the NUMECA suite, or the ANSYS CFX to estimate through the comparisons with the available experimental the level of accuracy of each of the two solvers. For the sake of similarity, in both cases the numerical simulation is based on the unsteady solution for the Reynolds-averaged Navier-Stokes (RANS hereafter) equations in which the turbulence is modeled with the k-ω SST model. The global hydrodynamic forces, moments and efficiency are computed for eight different advance coefficients to draw the open water diagram. A few introspections into the propeller freestream structure will be performed as well.

Keywords: numerical simulation**,** propeller, RANSE, open water test, turbulence

1. INTRODUCTION

The use of RANS methods for the simulation of the flow around ship hulls has already reached a first level of maturity. During the past two decades a consistent effort has been paid and spectacular progress has been reported not only in the development of robust, efficient and accurate codes, which are nowadays able to simulate free-surface flows dominated by viscous and turbulent features, but also in the development of novel techniques aimed at coping with the difficulties of the problem. The current methods can provide a promising accurate estimation of resistance, useful information for the ship hull form improvement, as well as valuable information on the flow features required by the necessity of designing the optimal propulsive systems. In order for all these tools to become fully reliable they should enter in industrial use. To do that, they still need to help the naval architect in solving certain problems such as the prediction of the propeller performances, including cavitation, the ship motions in incoming waves and the maneuverability that have appeared so far as being incompletely solved. Obviously there have already been reported several achievements in all the above mentioned fields but much effort has to be spent in the near future to validate the numeric tools to reach the level of confidence required by the industry.

Under all these circumstances, the present research focuses on the propulsion problem. Being a first step, the author only restricted to the open water case, without considering the cavitation, in the way of developing a robust and reliable technique for a

further investigation of the flow around a self-propelled ship hull.

The geometry of the studied propeller model was generously provided by the Japanese National Maritime Research Institute, which was one of organizers of the seventh Workshop on CFD in Ship Hydrodynamics organized in Tokyo [1]. The five-blade propeller considered in here was designed for the JBC hull. The National Maritime Research Institute, Yokohama National University and the Shipbuilding Research Centre of Japan were jointly involved in the design of the hull, the energy saving device and the rudder.

Towing tank experiments were carried out at NMRI, SRC and Osaka University, which include resistance tests, self-propulsion tests and PIV measurements of stern flow fields. The hull and propeller designs and measurements were performed with the support of Class Nippon Kaiji Kyokai as part of a R&D program as acknowledged in [2] and [3].

The reasons for choosing the JBC propeller model were two. The first one was given by the completeness of the experimental data the author needed for the verification and validation of the theoretical approach. The second one was given by the complexity of the propeller geometry shown in Fig.1, which usually raises additional difficulties especially for the pre-processing, when a large amount of effort is necessary to avoid unwanted defects such as twisted cells, lack of the orthogonality or of the grid smoothness.

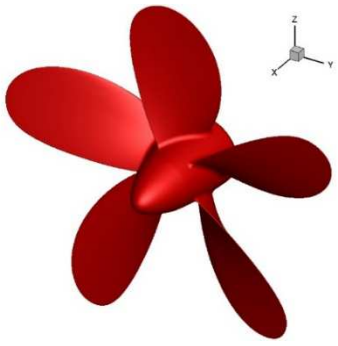

Fig. 1. Propeller geometry

The main particulars of the propeller model recommended in [1] are tabulated in Table 1.

Table1. Main particulars of the JBC propeller

Main particulars	value
Diameter [mm]	203.0
Boss ratio	0.180
Pitch (constant) [mm]	152.25
Pitch ratio	0.750
Expanded area ratio	0.500
Maximum blade width ratio	0.2262
Blade thickness ratio	0.050
Angle of rake	5^o
Number of blades	5
Blade section	au
Direction of rotation	clockwise

2. NUMERICAL APPROACH

There are a number of different solution methods that are used in CFD codes. One of the most commonly used is the finite volume technique, which is one the CFX is based on. In this technique, the region of interest is divided into small sub-regions, called control volumes. The equations are discretized and solved iteratively for each control volume. As a result, an approximation of the value of each variable at specific points throughout the domain can be obtained. In this way, one may derive a full picture of the behavior of the flow. The simulation is done in a global approach in which RANS equations written in respect to a Cartesian system of coordinates are numerically solved. A transient approach is used to advance the solution in time. The initial conditions refer to the incoming flow velocity, the propeller r.p.m. as well as to the pressure and turbulent viscosity.

The ISIS-CFD flow solver of the FINE^{TM}/Marine is also based on the finite volume method to build the spatial discretization of the transport equations [4]. The dependent variables of the set of equations are the velocity and pressure. To avoid the odd-even decoupling of pressure and velocity, a

third-order pressure smoothing is employed a Rhie and Chow [5] SIMPLE-type method: in each time step, the velocity updates come from the momentum equations and the pressure is given by the mass conservation law, transformed into a pressure equation. Diffusion terms are approximated using second-order central differences, whereas advective fluxes are approximated based on blends between high-order upwind-biased schemes.

The turbulence is treated by making use of the k-ω SST model in both simulation. The forces integration is performed on the solid-surface cell based on the quaternions formulation. The integration in time is done in an Euler explicit way, whereas an upwind discretization scheme is used for the convective terms with a second order for the acceleration. Conservation applies to the mass and momentum and a Piccard model applies for the linearization.

The pressure-correction is imposed and the Krylov technique is used for the iteration of the solution. An unstructured grid is used for the discretization of the computational domain and hexahedral elements are used for that purpose in ISIS-CFD, whereas a mix of tetrahedral and hexahedral elements are used in CFX. A quasistatic approach is used to advance the solution in time in ISIS-CFD, where the initial conditions refer to the incoming flow velocity, the propeller r.p.m. as well as to the pressure and turbulent viscosity.

In both cases the computational domain is approximated by a cylinder with a radius equal to 1.75 the propeller diameter, as Fig.2 shows. The computational domain is limited at 2 diameters at the upstream of the propeller where the streamwise and lateral components of velocity, the pressure and the turbulent viscosity are imposed, whereas a Neumann condition is imposed for the pressure. At the downstream, which is located at 3 diameters from the propeller, the velocity components and the turbulent viscosity are zero-extrapolated, whereas the pressure has the static value. The no-slip condition is imposed on the propeller and the shaft, while the zero gradient is imposed on the external boundary for all the parameters. The flow starts from rest and it is accelerated within 5 seconds up to the given incoming velocity.

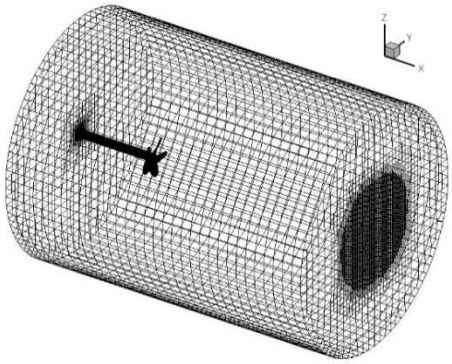

Fig. 2. Computational domain

2.1 GRID GENERATION

For the ISIS-CFD solver, the propeller geometry provided by NMRI was converted to a PARASOLID file and the grid was built in HEPRESS, a grid generator which has not only direct CAD import capabilities, but it also allows the manipulation or the decomposition of the geometry. For the CFX the grid was constructed by making use of its own mesh generator. Fig. 3 shows the details of the surface grid.

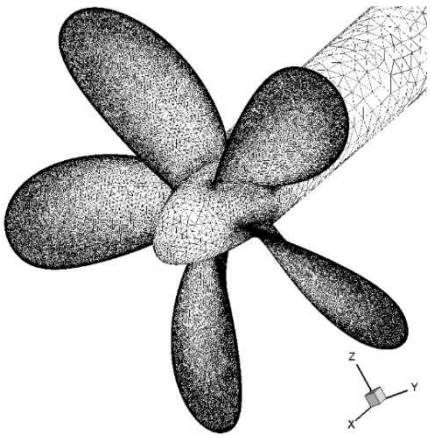

Fig. 3. Computational grid on the propeller

Since the problem to solve refers to a flow at a high Reynolds number, therefore it is expected to deal with a very thin boundary layer next to the solid walls of the domain. To establish correctly the cell size inside the boundary layer, the wall variable y^+ is imposed at a value which is less than 5. An automatic refinement procedure based on defined sensors either next to solid walls or inside specified area in the domain is used on both cases of computations [6]. Grids of about 6 million cells were generated for each solver.

3. RESULTS AND DISCUSSIONS

All the computations are carried out at an inflow velocity of 1.978 m/s, for which eight different angular speeds are considered for the propeller so that advance coefficients result in between 0.1 and 0.8 for which the experimental data are available. The corresponding propeller revolution was between 727 and 5800 r.p.m. The solution was computed for 10 seconds in both cases, either on a computer with 12 cores, or on an HPC with 624 cores, so that the propeller could perform at least 121 revolutions for the largest advance coefficient, *J*. It is important to mention that the time evolutions of the thrust and torque depicted in Figs. 4 and 5 prove that the solution computed with the ISIS-CFD solver converges rather quickly after the acceleration period.

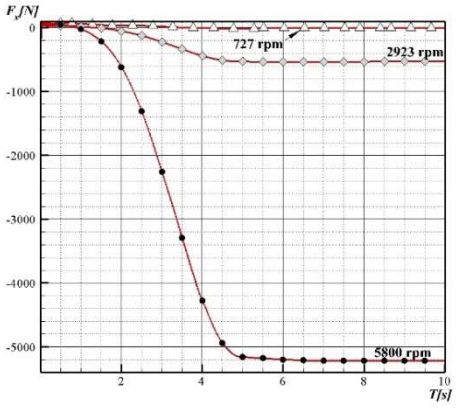

Fig. 4. Time variation of the thrust computed for three different revolutions

The explanation for the negative values for the thrust is that the incoming flow velocity direction was initially set towards the positive direction of the *x*-axis, so the hydrodynamic force is oriented in the opposite direction. Similarly, the torque is positive since the propeller rotation is clockwise.

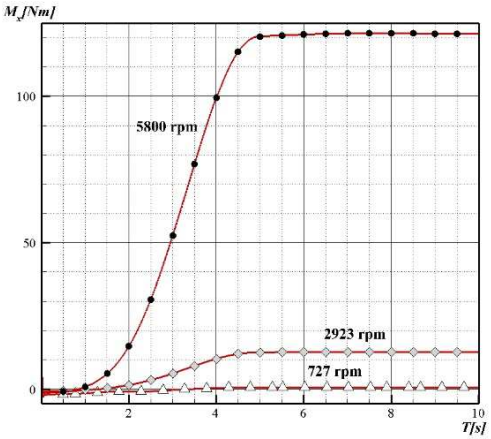

Fig. 5. Time variation of the torque computed for three different revolutions

Since the most important issue of any transient or quasisteady simulation is the correlation between the time discretization and the grid size, the time step was 10^{-4} so that the Courant number remained below the unity. In the following a series of qualitative discussions will be made upon the solutions computed with the ISIS-CFD solver only.

The reason for the author's choice resides in the necessity to test the capability of the numerical tool to accurately describe the flow around propellers prior to perform self-propulsion numerical simulations. No quantitative assertions will be made because of the missing experimental data.

Fig.6 shows the pressure distribution on the two faces of the propeller blades computed for the 5800 r.p.m. case, at T=10s . The pressure is higher on the pressure side and around the leading edge of the hydrodynamic profile, see Fig.6 (a), a fact which is confirmed by the propeller theory. On the opposite, the suction side, Fig.6 (b), displays areas of lower pres-

sure which are located around the middle chord and towards the tip of the blades.

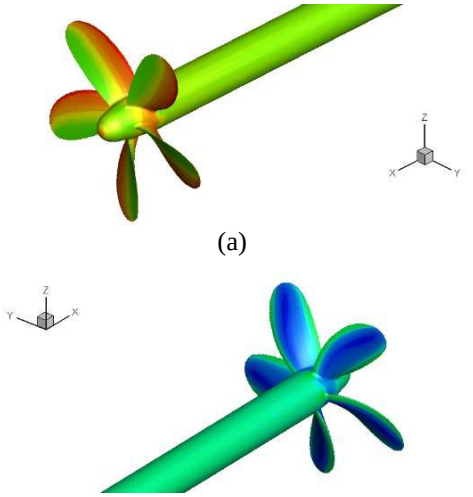

(a)

(b)

Fig. 6. Pressure distribution on the two faces of the propeller blades computed with ISIS-CFD at T=10s

Fig.7 shows the velocity components distribution on the propeller blades computed with ISIS-CFD at T=10s in the 5800 r.p.m. case. Fig 7(a) depicts the streamwise component contours. The velocity is smaller along the leading edge because of the stagnation that takes place in that area. On the opposite, the flows accelerate towards the trailing edge of the chord as the figure proves. The contours for the computed lateral and vertical components show in Figs.7 (a) and (b) are antisymmetric in respect to the corresponding axes of the Cartesian system of coordinates, as expected. Another important hydrodynamic parameter for the flow around the propeller is related to the vortical character of the flow. In such respect Fig.8 shows the streamwise velocity field in the propeller plane computed at T=10s in the 2923 r.p.m. case. As depicted in the figure, on the pressure side of the blade, along the leading edge, there is a region of high axial velocity, which explains the formations of the vortices, as it will be discussed later on.

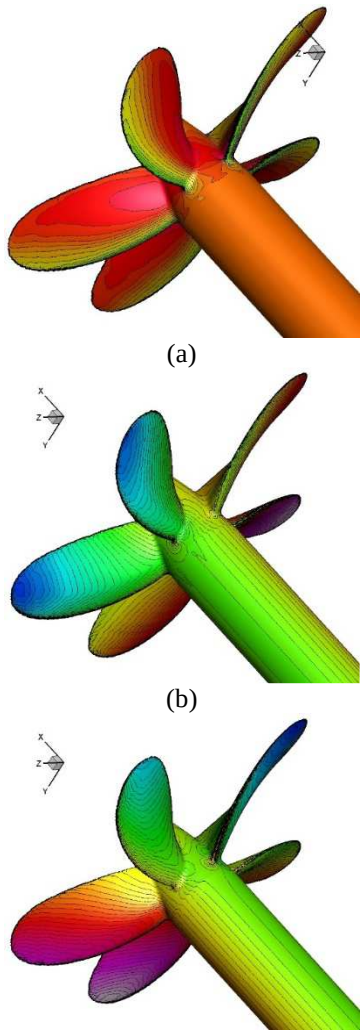

(a)

(b)

(c)

Fig. 7. Velocity components distribution on the propeller blades computed with ISIS-CFD at T=10s

The same conclusion is valid for the propeller working at 727 r.p.m. although the intensity of the peaks is smaller. This can be seen in Fig.9 which shows the streamwise velocity distribution in the vertical plane of the propeller shaft computed at T=10s. Apart of the Eulerian velocity gradient tensor, which does not always give significant information, the CFD literature recommends for the vortex core prediction the use of

either pathline and streamline, or the use of the vorticity. Nevertheless, it seems that methods based on the use of the second variant and the helicity or vorticity.

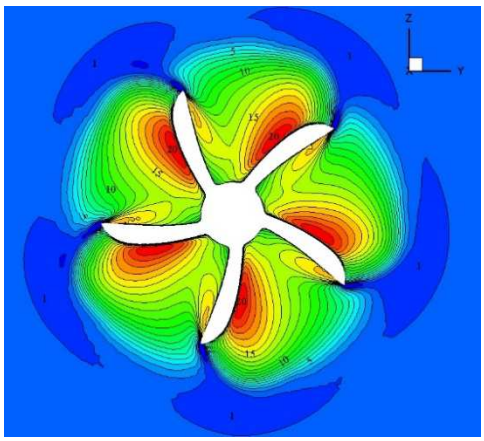

Fig. 8. Vorticity distribution in the transversal plane of the propeller computed for the 2923 r.p.m. case with ISIS-CFD at T=10s

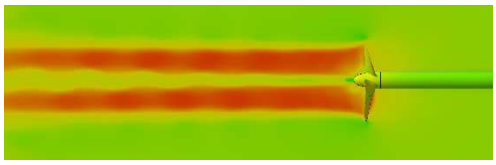

Fig. 9. Streamwise velocity distribution in the vertical plane of the propeller shaft computed for the 727 r.p.m. with ISIS-CFD at T=10s

The second variant criterion, which works efficiently whenever one wants to visualize the vortex core, is based on the critical point analysis for velocity gradient tensor [7]. Therefore, to get more insight in the vortex generation formation, an analysis based on the Q^* criterion is proposed [8]. The criterion is defined as:

$$Q^* = Q\frac{D^2}{U_{ref}^2}$$

where D is the propeller diameter and Q is the computed second invariant.

Following the procedure proposed by Visonneau et al. in [9], Fig. 10 depicts the isosurface of $Q^* = 50$ plotted in the propeller wake and colored by the non-dimensional helicity. The isosurface plot provides a valuable information concerning the core of the vortices which are developed in the stream. Obviously the flow behind the propeller has two vortices, one which originates from the tip of the blade, while the other is the hub vortex.

The intensity of the tip vortex is stronger than that of the other. Their intensity is significant immediately in the propeller wake and decreases as the vortices are washed down in the stream. Aside of that, the spiral on which the cores are placed suffers an increase in the diameter because of the viscous diffusion.

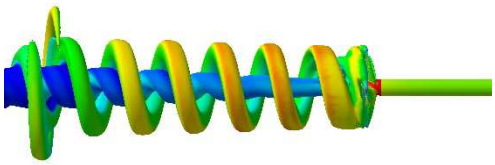

Fig. 10. Vortices cores in the propeller wake

In the following a comparison between the open water diagrams computed with ISIS-CFD and CFX at T=10s and measured [3] is proposed in Fig.11. At first glance, the resemblance between the computed data and the measured one shows a good agreement. Since both computations were performed on grids with almost the same number of cells, one may say that both solvers behave similarly. However there are some differences which will be discussed in every detail the followings.

From the point of view of the accuracy of the solution, CFX seems to be closer to the experimental data, i.e., the maximum error was 2.16%, whereas in the ISIS-CFD computations went to 3.02%. The departure from the EFD data was larger for all K_T, K_Q and η, respectively. The required CPU time till the convergence was 34.23% lower for the ISIS-CFD computed solution. In terms of the hardware requirements, CFX proved to need less resources, especially in terms of the needed disk space, which was about 20% smaller.

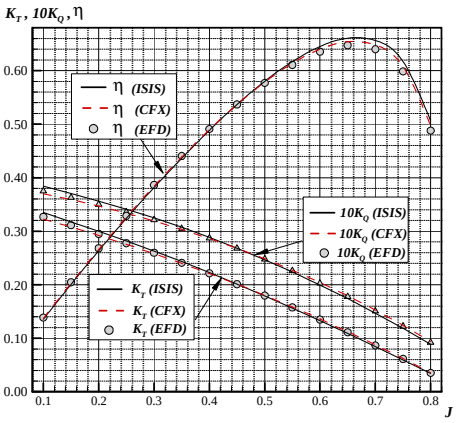

Fig. 11. Comparisons between the open water diagrams computed with ISIS-CFD and CFX at T=10s and measured [3]

4. CONCLUDING REMARKS

The paper describes a 3D numerical simulation of the viscous flow around a five blade propeller model, as an intermediate step in developing a robust technique for a further investigation of the flow around a self-propelled ship hull. Several computations were performed by using either the FINE^{TM}/Marine component of the NUMECA suite, or the ANSYS CFX to estimate through the comparisons with the available experimental the level of accuracy of each of the two solvers.

For the sake of similarity, in both cases the numerical simulation is based on the unsteady solution for the Reynolds-averaged Navier-Stokes (RANS hereafter) equations in which the turbulence is modeled with the k-ω SST model. The global hydrodynamic forces, moments and efficiency are computed for eighth different advance coefficients to draw the open water diagram.

The simulation is accomplished in a global approach in which the solution for the RANS equations written in respect to a Cartesian system of coordinates is advanced in time in a classical Euler manner.

Both CFX and ISIS-CFD flow solvers are based on the finite volume method to build the spatial discretization of the transport equations. The dependent variables of the set of equations are the velocity and pressure.

Eight set of parallel computations were performed and the solutions were compared with EFD data [3] existent on the public domain and the main conclusions are as followings:

- the resemblance between the computed and the EFD data shows a good agreement;
- both computations were performed on grids with almost the same number of cells, therefore it may be concluded that both solvers worked well;
- from the point of view of the accuracy of the solution, CFX seems to be closer to the experimental data, i.e., the maximum error was 2.16%, whereas in the ISIS-CFD computations went to 3.02%, so the CFX is more accurate;
- the CPU time till the convergence was 34.23% lower for the ISIS-CFD computed solution. From this point of view it may be concluded that the solver is more efficient;
- the CFX proved to need less hardware resources, especially in terms of the needed disk space, which was about 20% smaller.

Since the final goal of any numerical investigation of the ship hydrodynamics is to simulate the motions of a self-propelled hull moving freely on a free-surface water, it seems that the choice for the further investigations should be the ISIS-CFD solver of the FINE^{TM}/Marine package in spite of some of its drawbacks.

REFERENCES

[1]. **NMRI** (2015), *"Tokyo 2015 A Workshop on CFD in Ship Hydrodynamics"*, retrieved from http://www.t2015.nmri.go.jp/

[2]. **Hirata, N.,** http://www.t2015.nmri.go.jp/Presentations/Day1-AM2-JBC-TestData1-Hirata.pdf

[3]. **Hino, T.,** http://www.t2015.nmri.go.jp/Presentations/Day2-AM1-JBC-SpinclESD-Hino.pdf

[4]. **Wackers, J., Koren, B., Raven, H.C., van der Ploeg, A., Starke, A.R., Deng, G.B., Queutey, P., Visonneau, M., Hino, T., Ohashi, K.,** *"Free-Surface Viscous Flow Solution Methods for Ship Hydrodynamics"*, Archives of Computational Methods in Engineering, (18) pp. 1–41, 2011.

[5]. **Rhie, C.M., Chow, W. L.,** *"A Numerical Study for the Turbulent Flow an Isolated Airflow with Trailing Edge Separation"*, AIAA Journal,1983 (**17**), pp. 1525, 1983.

[6]. **Wackers, J., Deng, G.B., Guilmineau, E., Leroyer, A., Queutey, P., Visonneau, M.,** (2014), *"Combined Refinement Criteria for Anisotropic Grid Refinement in Free-Surface Flow Simulation"*, Computers and Fluids, 92, 209–222, 2014.

[7]. **Jeong, J., Hussain, F.,** *"On the Identification of a Vortex"*, Journal of Fluid Mechanics, Vol. 285, pp. 69-94, 1995

[8]. **Deng, G.B., Leroyer, A., Guilmineau, E., Queutey, P., Visonneau, M., Wackers, J., del Toro Llorens, A.,** *"Verification and Validation of Resistance and Propulsion Computation"*, Proceedings of Tokyo 2015 Workshop on CFD in Ship Hydrodynamics, 2015.

[9]. **Visonneau, M., Deng, G.B., Guilmineau, E., Queutey, P., Wackers, J.,** *"Local and Global Assessment of the Flow around the Japanese Bulk Carrier with and without Energy Saving Devices at Model and Full Scale"*, Proceedings of the 31st Symposium on Naval Hydrodynamics, Monterey, California, 2016.

Paper received on November 5th, 2016

